1-2010

Finite Element Analysis of Ring-Shaped Emission Profile in Plasma Bullet

Yukinori Sakiyama

David B. Graves

Julien Jarrige
Old Dominion University

Mounir Laroussi
Old Dominion University, mlarouss@odu.edu

Original Publication Citation

Sakiyama, Y., Graves, D.B., Jarrige, J., & Laroussi, M. (2010). Finite element analysis of ring-shaped emission profile in plasma bullet. *Applied Physics Letters, 96*(041501), 1-3. doi: 10.1063/1.3298639

Finite element analysis of ring-shaped emission profile in plasma bullet

Yukinori Sakiyama, David B. Graves, Julien Jarrige, and Mounir Laroussi

Citation: Applied Physics Letters **96**, 041501 (2010); doi: 10.1063/1.3298639
View online: http://dx.doi.org/10.1063/1.3298639
View Table of Contents: http://scitation.aip.org/content/aip/journal/apl/96/4?ver=pdfcov
Published by the AIP Publishing

Finite element analysis of ring-shaped emission profile in plasma bullet

Yukinori Sakiyama,[1,a)] David B. Graves,[1] Julien Jarrige,[2] and Mounir Laroussi[2]
[1]*Department of Chemical Engineering, University of California, Berkeley, California 94720, USA*
[2]*Laser and Plasma Engineering Institute, Old Dominion University, Norfolk, Virginia 23529, USA*

(Received 23 September 2009; accepted 5 January 2010; published online 26 January 2010)

Using a one-way coupled model of neutral gas flow and plasma dynamics we report a mechanism to explain the ring-shaped emission pattern that has been observed experimentally in plasma bullets at atmospheric pressure. We solve a fluid model with the local field approximation in one-dimensional cylindrical coordinates, corresponding to a cross-section of a plasma bullet. Pulselike uniform electric field is assumed to be applied perpendicular to the simulation domain. Time and spatially resolved spectroscopic measurements support the simulation results. © *2010 American Institute of Physics*. [doi:10.1063/1.3298639]

Several research groups demonstrated that atmospheric pressure plasma jets are not continuous jets but discrete fast-moving plasma packets or bullets.[1–4] The discharge mechanisms are however not fully understood. Lu and Laroussi[2] proposed a photoionization model. Sands *et al.*[3] reported that plasma jets exhibit properties similar to positive streamers. More interestingly, cross-sectional images of jets show ring-shaped emission pattern, corresponding to a hollow structure.[1,5] In this study, we focus on modeling of the ring-shaped emission patterns.

We employed a one-way coupled model between neutral gas flow and plasma dynamics. The models are solved using COMSOL[6] with MATLAB.[7] The steady state neutral gas flow model describes convection of helium gas flow and air back-diffusion into helium flow in two-dimensional cylindrical coordinates. The "air" in the current model is assumed to be pure nitrogen to avoid complicated oxygen plasma chemistry. The governing equations for the neutral gas flow consist of total mass continuity equation, momentum continuity equation (i.e., compressible Navier–Stokes equation), and mass continuity equation for nitrogen. The temperature of the background gas is fixed at 300 K. More detailed discussion and formulation of neutral gas flow equations are given in Ref. 8. Figure 1 shows simulation results of two-dimensional distribution of mole fraction of nitrogen. A tube plasma reactor is located near the left bottom corner of the simulation domain. A fully developed laminar flow (i.e., Poiseuille flow) enters the domain at $z=-20$ mm with flow rate of 7 l/min. Our model clearly shows that helium-rich region stretches over 50 mm near the axis of symmetry. Nitrogen concentration rapidly increases in radial direction due to diffusion, thus creating a narrow helium channel. In the following sections, we discuss the plasma structure at two different cross-sections: an upstream point ($z=20$ mm) and a downstream point ($z=40$ mm). Background gas composition is kept constant as shown in the inset graph in Fig. 1.

Our time-dependent plasma model is based on a fluid model with the local field approximation in one dimensional cylindrical coordinates. The simulation region corresponds to a cross section of a plasma bullet (i.e., r direction in Fig. 1). The plasma model is almost identical to our previous report,[9] which includes six different species and 13 elementary reactions. The governing equations consist of Poisson's equation in radial direction and species continuity equations with the drift-diffusion approximation for electrons, heavy positive ions, and metastables. The major difference is that the current model includes nitrogen metastable N_2 $(C^3\Pi)$ and three additional reactions as follows: $N_2+e\rightarrow N_2(C^3\Pi)+e$, $N_2+e\rightarrow N_2^+ +e$, and N_2 $(C^3\Pi)\rightarrow N_2+h\nu$ [$k=2.45\times10^7$ s^{-1} (Ref. 10)]. In addition, we reconstructed look-up tables for electron impact reactions and electron transport coefficients so that the coefficients are expressed as functions of both the local electric field and the mole fraction of nitrogen. Another important difference is that pulselike uniform electric field ($\mathbf{E}_z$) is given perpendicular to the simulation domain (i.e., z direction in Fig. 1). The pulse consists of a 200 ns flat plateau and 100 ns rise/decay time. The pulse duration was estimated from the duration of conduction current carried by a bullet in Ref. 2. We note that the pulselike electric field does not represent the applied voltage pulse in our experiment described later. The repetition frequency is 8 kHz. The magnitude of the electric field (3×10^5 $\mathrm{V/m}$) is uniform in r direction and chosen so that a periodic steady state solution can be obtained. Thus, the current plasma model is not self-consistent though we solve Poisson's equation in r direction. The equation system reaches a periodic steady state in ten cycles, starting from uniform and low particle density ($\sim10^{12}$ m^{-3}).

Figure 2 show instantaneous distributions of electron densities and ionization rate at $z=20$ mm at the end of the rise of the pulselike electric field ($t=100$ ns) and at the beginning of the decay of the pulselike electric field ($t=300$ ns). In the early stage ($t=100$ ns), the discharge is substantially sustained by electron impact ionization of helium. The density of electrons and ions shows relatively broad peaks near the center ($r=0$) though the applied electric field $\mathbf{E}_z$ is uniform. Interestingly, Penning ionization between helium metastables and background nitrogen shows the peak around $r=0.4$ mm. In addition, the peak of nitrogen metastable density is observed at off-centered position

a)Electronic mail: ysaki@berkeley.edu.

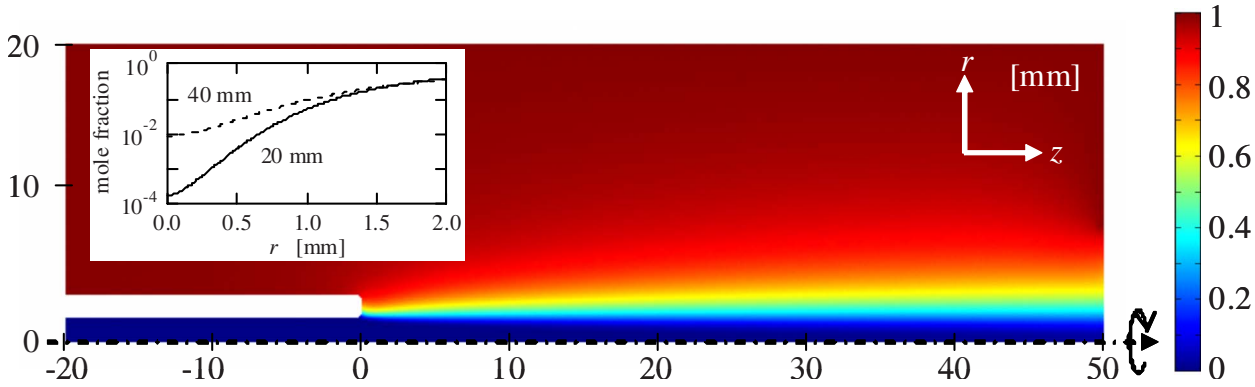

FIG. 1. (Color online) Two-dimensional distribution of mole fraction of nitrogen. The inset graph shows mole fraction of nitrogen in radial direction at z =20 and 40 mm.

(r=0.5 mm) although we do not show the plot here. These are explained by the sharp gradient of nitrogen density as shown in Fig. 1. Nitrogen density near the center is significantly low, whereas nitrogen density far away from the center is so high that electron energy is quenched. Consequently, nonuniform distribution of electron impact excitation/ionization rate is formed in the simulation domain. Penning ionization plays only minor role in sustaining the plasma at the early stage of the discharge (t=100 ns). Through nonlinear electron multiplication process, however, the off-centered Penning ionization peak eventually generates off-centered peak of electron density in the late stage of the discharge (t=300 ns).

We performed spectroscopic measurements to investigate the structure of the plasma bullets and to compare with the simulation results. A schematic diagram of the experimental setup is shown in Fig. 3. The plasma jet was generated by a dielectric barrier discharge reactor in a cylindrical configuration. The reactor was made of an acrylic tube with an internal diameter of 3 mm and a thickness of 1.5 mm. The electrodes consist of two copper foils wrapped around the tube. The reactor was driven by a unipolar positive high voltage pulse forming system. The pulse amplitude was 7 kV, the pulse width 2 μs, and the repetition frequency 8 kHz. The rise time and fall time were around 40 ns. The discharge reactor was fed with pure helium and the flow rate was fixed at 7 l/min using mass flow controllers. These conditions are close to the simulation conditions described above. The plasma jet propagating in ambient air was characterized by optical emission spectroscopy. We used a monochromator (Spectra Pro 500i, Acton Research) with a grating of 3600 grooves/mm and a photomultiplier tube (PD-471, Roper Scientific). The relative density of N_2 ($C^3\Pi_u$) and N_2^+ ($B^2\Sigma_u^+$) were obtained using the intensity of, respectively, 0–0 band of N_2 second positive system (SPS) at 337.1 nm, and 0–0 band of N_2^+ first negative system (FNS) at 391.2 nm. The spatial distribution of N_2 (C) was determined by measuring the intensity of SPS at different radial positions. The radial profile was then calculated using Abel inversion method.

Figure 4 shows spatially resolved emission profiles from N_2 SPS, upstream (z=20 mm) and downstream (z=40 mm). Light emission from nitrogen clearly shows an off-centered peak at the upstream point. On the other hand, the emission profile shifts to the center and the ring-shape almost collapses at the downstream point. Our plasma model reproduces the experimental observation. Both experiments and simulation indicate that the diameter of the plasma bullet

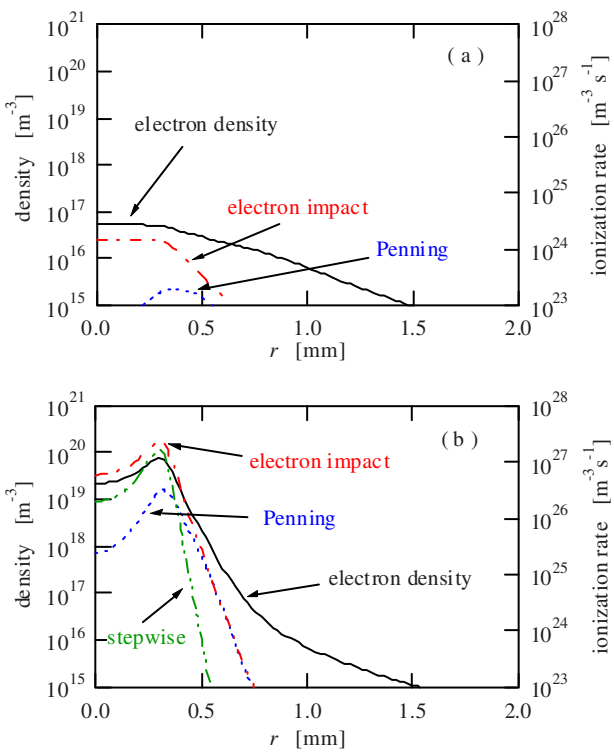

FIG. 2. (Color online) Instantaneous distribution of electron density (left axis) and various ionization rates (right axis) at z=20 mm (a) at 100 ns and (b) 300 ns.

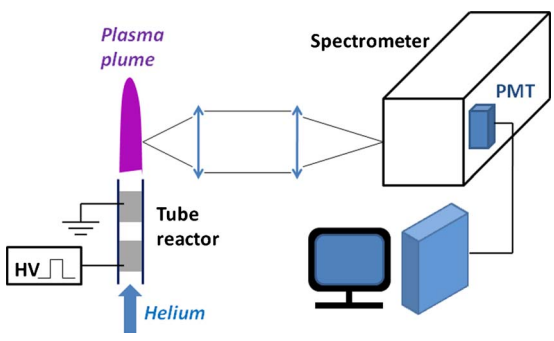

FIG. 3. (Color online) A schematic diagram for spectroscopic measurement.

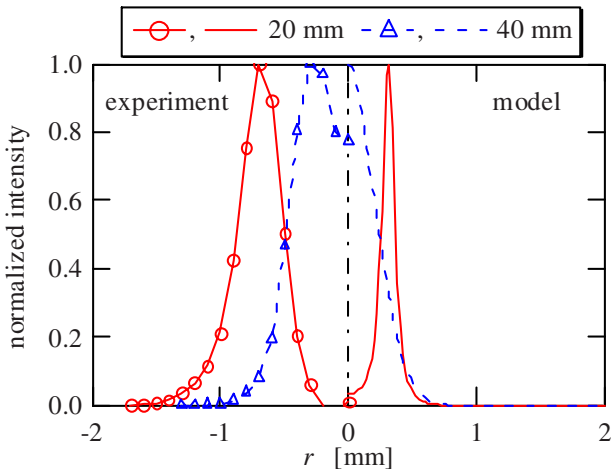

FIG. 4. (Color online) Time-averaged relative emission profiles from N_2 SPS. The right half shows simulation results and the left half experimental results. The solid lines and circles are results at $z=20$ mm and the triangles and dashed lines are at 40 mm.

decreases as it propagates away from the tube exit. This is consistent with previous experimental observations by Lu and Laroussi[2] and Begum *et al.*[11] Again, the off-centered peaks are due to diffusion of air (nitrogen) into the helium flow as we discussed above.

Figures 5(a) and 5(b) show a comparison of time-resolved emission intensity from helium, nitrogen, and nitrogen ion at the upstream point ($z=20$ mm) between experiment and modeling. In Fig. 5(b), we plot electron impact ionization rate of helium as an indicator of emission from helium. The sum of Penning ionization and charge transfer reaction are used as an indicator of emission from nitrogen ion.[12] Our experimental observation shows that at a fixed point emission from helium is observed first, followed by emission from nitrogen and nitrogen ion. The simulation results qualitatively agree with the measurement. Our model indicates the delay between emission from helium and from nitrogen/nitrogen ion is due to difference in electron impact reaction rate. We think discrepancy in the decay time of emission from nitrogen ion is due to the simplified chemistry model, especially lack of oxygen. Also the current one-dimensional model is unable to reproduce the small "bump" between 100 and 200 ns observed by our experiments. This could come from two-dimensional effects of the bullet and/or nonuniformity of the electric field. We however emphasize that the non-self-consistent plasma model we report here is capable of capturing many essential features of the plasma bullet, which have been experimentally validated.

In summary, our one-way coupled model of neutral gas flow and plasma dynamics shows that air diffusion against helium convection creates the unique ring-shape emission profile in atmospheric pressure plasma bullets. Our spectroscopic measurements support the simulation results. It is

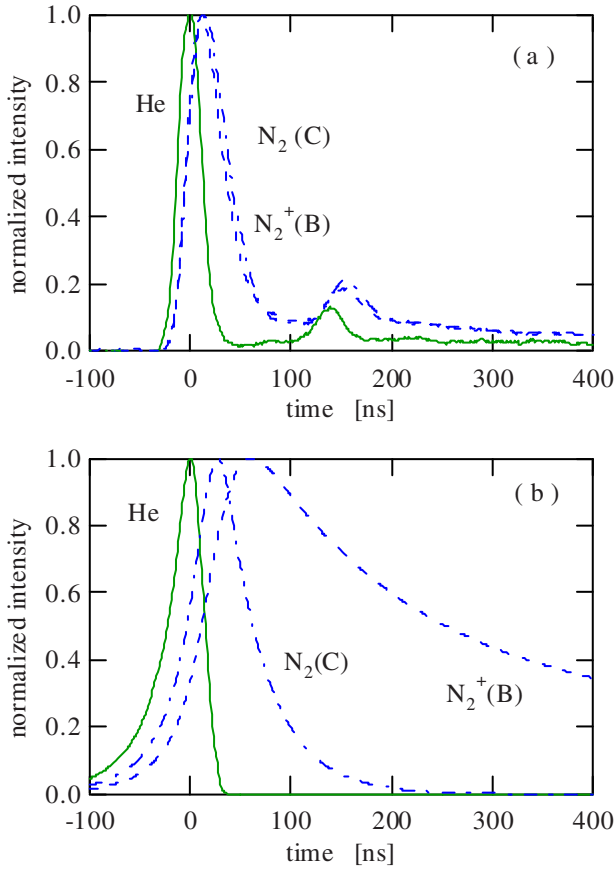

FIG. 5. (Color online) Time-resolved emission profile at $(r,z)=(0,20)$ of helium, nitrogen, and nitrogen ion by (a) experiment and (b) simulation. The origin of time is the moment when emission from helium shows the peak value.

worth noting that the discharge mechanisms are analogous to the plasma needle discharge although the discharge conditions are different.[13]

[1]M. Teschke, J. Kedzierski, E. G. Finantu-Dinu, D. Korzec, and J. Engemann, IEEE Trans. Plasma Sci. **33**, 310 (2005).
[2]X. P. Lu and M. Laroussi, J. Appl. Phys. **100**, 063302 (2006).
[3]B. L. Sands, B. N. Ganguly, and K. Tachibana, Appl. Phys. Lett. **92**, 151503 (2008).
[4]J. Shi, F. Zhong, J. Zhang, D. W. Liu, and M. G. Kong, Phys. Plasmas **15**, 013504 (2008).
[5]N. Mericam-Bourdet, M. Laroussi, A. Begum, and E. Karakas, J. Phys. D **42**, 055207 (2009).
[6]COMSOL 3.5a (COMSOL, Burlington, MA, 2008).
[7]MATLAB 7.4 (Mathworks, Natick, MA, 2007).
[8]R. B. Bird, W. E. Stewart, and E. N. Lightfoot, *Transport Phenomena* (Wiley, New York, 2002).
[9]Y. Sakiyama and D. B. Graves, J. Phys. D **39**, 3644 (2006).
[10]M. Capitelli, C. M. Ferreira, B. F. Gordiets, and A. I. Osipov, *Plasma Kinetics in Atmospheric Gases* (Springer, Berlin, 2000).
[11]A. Begum, E. Karakas, and M. Laroussi, 61st Annual Gaseous Electronics Conference, p. 47, Dallas, TX, October 2008.
[12]Y. Sakiyama, D. B. Graves, and E. Stoffels, J. Phys. D **41**, 095204 (2008).
[13]Y. Sakiyama and D. B. Graves, Plasma Sources Sci. Technol. **18**, 025022 (2009).